Euler's disk and its finite-time singularity

Air viscosity makes the rolling speed of a disk go up as its energy goes down.

It is a fact of common experience that if a circular disk (for example, a penny) is spun upon a table, then ultimately it comes to rest quite abruptly, the final stage of motion being characterized by a shudder and a whirring sound of rapidly increasing frequency. As the disk rolls on its rim, the point P of rolling contact describes a circle with angular velocity Ω. In the classical (non-dissipative) theory[1], Ω is constant and the motion persists forever, in stark conflict with observation. Here I show that viscous dissipation in the thin layer of air between the disk and the table is sufficient to account for the observed abruptness of the settling process, during which, paradoxically, Ω increases without limit. I analyse the nature of this 'finite-time singularity', and show how it must be resolved.

Let α be the angle between the plane of the disk and the table. In the classical description, and with the notation defined in Fig. 1, the points P and O are instantaneously at rest in the disk, and the motion is therefore instantaneously one of rotation about line PO with angular velocity ω, say. The angular momentum of the disk is therefore $\mathbf{h} = A\omega\mathbf{e}(t)$, where $A = \frac{1}{4}Ma^2$ is the moment of inertia of the disk of mass M about its diameter; $\mathbf{e}(t)$ is a unit vector in the direction PO; $\mathbf{e}_z$, $\mathbf{e}_d$ are unit vectors in the directions Oz, OC, respectively (see Fig. 1). In a frame of reference rotating with angular velocity $\Omega_d = \Omega\mathbf{e}_z$, the disk rotates about its axis OC with angular velocity $\Omega_d = \Omega_d\mathbf{e}_d$; hence the rolling condition is $\Omega_d = \Omega\cos\alpha$. The absolute angular velocity of the disk is thus $\omega = \Omega(\mathbf{e}_d\cos\alpha - \mathbf{e}_z)$, and so

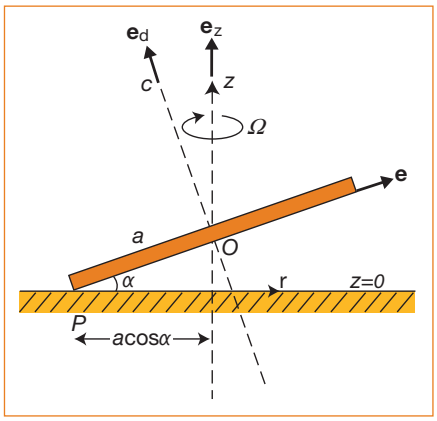

Figure 1 A heavy disk rolls on a horizontal table. The point of rolling contact P moves on a circle with angular velocity Ω. Owing to dissipative effects, the angle α decreases to zero within a finite time and Ω increases in proportion to $\alpha^{-1/2}$.

$$\omega = \boldsymbol{\omega}\cdot\mathbf{e} = -\Omega\sin\alpha.$$

Euler's equation for the motion of a rigid body is here given by $\mathrm{d}\mathbf{h}/\mathrm{d}t = \boldsymbol{\Omega}\wedge\mathbf{h} = \mathbf{G}$, where $\mathbf{G} = Mga\mathbf{e}_z\wedge\mathbf{e}$ is the gravitational torque relative to P ($\wedge$ indicates the vector product). This immediately gives the result $\Omega^2\sin\alpha = 4g/a$, or, when α is small,

$$\Omega^2\alpha \approx 4g/a \qquad (1)$$

The energy of the motion E is the sum of the kinetic energy $\frac{1}{2}A\omega^2 = \frac{1}{2}Mga\sin\alpha$, and the potential energy $Mga\sin\alpha$, so

$$E = \tfrac{3}{2}Mga\sin\alpha \approx \tfrac{3}{2}Mga\alpha \qquad (2)$$

In the classical theory, α, Ω and E are all constant, and the motion continues indefinitely. As observed above, this is utterly unrealistic.

Let us then consider one of the obvious mechanisms of energy dissipation, namely that associated with the viscosity μ of the surrounding air. When α is small, the dominant contribution to the viscous dissipation comes from the layer of air between the disk and the table, which is subjected to strong shear when Ω is large. We may estimate the rate of dissipation of energy in this layer as follows. Let (r,θ) be polar coordinates with origin at O. For small α, the gap $h(r,\theta,t)$ between the disk and the table is given by $h(r,\theta,t) \approx \alpha(a + r\cos\phi)$, where $\phi = \theta - \Omega t$. We now concede that α is a slowly varying function of time t: we assume that $|\dot{\alpha}| \ll \Omega$, and make the 'adiabatic' assumption that equation (1) continues to hold. Because the air moves a distance of order a in a time $2\pi/\Omega$, the horizontal velocity $\mathbf{u}_H$ in the layer has order of magnitude $r\Omega\sin\phi$; and as this velocity satisfies the no-slip condition on $z = 0$ and on $z = h$ ($= O(\alpha a)$), the vertical shear $|\partial\mathbf{u}_H/\partial z|$ is of the order $(r\Omega/\alpha a)|\sin\phi|$. The rate of viscous dissipation of energy Φ is given by integrating $\mu(\partial\mathbf{u}_H/\partial z)^2$ over the volume V of the layer of air: this easily gives $\Phi \approx \pi\mu g a^2/\alpha^2$, using equation (1). The fact that $\Phi \to \infty$ as $\alpha \to 0$ should be noted.

The energy E now satisfies $\mathrm{d}E/\mathrm{d}t = -\Phi$ (neglecting all other dissipation mechanisms). Hence, with E given by equation (2), it follows that

$$\tfrac{3}{2}Mga\,\mathrm{d}\alpha/\mathrm{d}t \approx -\pi\mu g a^2/\alpha^2 \qquad (3)$$

This integrates to give

$$\alpha^3 = 2\pi(t_0 - t)/t_1 \qquad (4)$$

where $t_1 = M/\mu a$, and t_0 is a constant of integration determined by the initial condition: if $\alpha = \alpha_0$ when $t = 0$, then $t_0 = (\alpha_0^3/2\pi)t_1$. What is striking here is that, according to equation (4), α does indeed go to zero at the finite time $t = t_0$. The corresponding behaviour of Ω is $\Omega \approx (t_0 - t)^{-1/6}$, which is certainly singular as $t \to t_0$.

Of course, such a singularity cannot be realized in practice: nature abhors a singularity, and some physical effect must intervene to prevent its occurrence. Here it is not difficult to identify this effect: the vertical acceleration $|\ddot{h}| = |a\ddot{\alpha}|$ cannot exceed g in magnitude (as the normal reaction at P must remain positive). From equation (4), this implies that the above theory breaks down at a time τ before t_0, where

$$\tau = t_0 - t \approx (2a/9g)^{3/5}(2\pi/t_1)^{1/5} \qquad (5)$$

A toy, appropriately called Euler's disk[2], is commercially available (Fig. 2; Tangent Toys, Sausalito, California). For this disk, $M = 400$ g, and $a = 3.75$ cm. With these values and with $\mu = 1.78\times10^{-4}$ g cm^{-1} s, $t_1 = M/\mu a \approx 0.8\times10^6$ s, and, if we take $\alpha_0 = 0.1 (\approx 6°)$, we find $t_0 \approx 100$ s. This is indeed the order of magnitude (to within $\pm 20\%$) of the observed settling time in many repetitions of the spinning of the disk (with quite variable and ill-controlled initial conditions), that is, there is no doubt that dissipation associated with air friction is sufficient to account for the observed behaviour. The value of τ given by equation (5) is 10^{-2} s for the disk values given above; that is, the behaviour described by equation (4) persists until within 10^{-2} s of the singularity time t_0. At this stage, $\alpha \approx 0.5\times10^{-2}$, $h_0 = a\alpha \approx 0.2$ mm, $\Omega \approx 500$ Hz (and the adiabatic approximation is still well

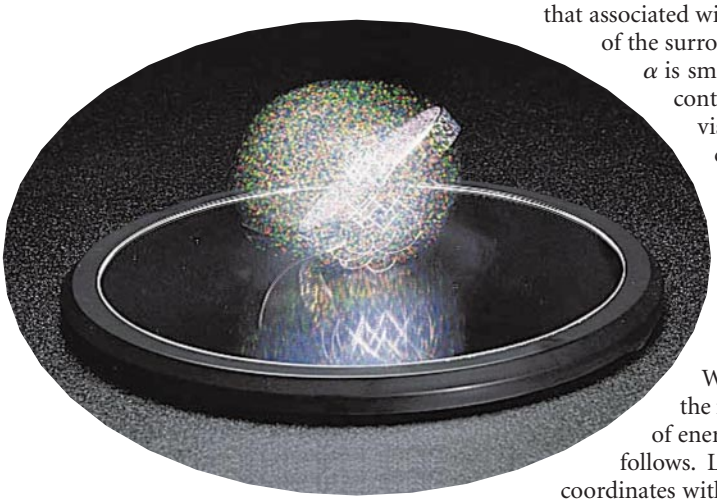

Figure 2 Euler's disk is a chrome-plated steel disk with one edge machined to a smooth radius. If it were not for friction and vibration, the disk would spin for ever. Photo courtesy of Tangent Toys. See http://www.tangenttoy.com/.

satisfied). This is as near to a 'singularity' as this simple toy can approach. The effect is nevertheless striking in practice.

H. K. Moffatt
Isaac Newton Institute for Mathematical Sciences, 20 Clarkson Road, Cambridge CB3 0EH, UK
e-mail: hkm2@newton.cam.ac.uk

1. Pars, L. A. *Treatise on Analytical Dynamics* (Heinemann, London, 1965).
2. Euler, L. *Theoria Motus Corporum Solidorum Seu Rigidorum* (Greifswald, 1765).

Molecular transistors

Potential modulations along carbon nanotubes

True molecular-scale transistors have been realized using semiconducting carbon nanotubes[1–5], but no direct measurements of the underlying electronic structure of these have been made. Here we use a new scanning-probe technique to investigate the potential profile of these devices. Surprisingly, we find that the potential does not vary in a smooth, monotonic way, but instead shows marked modulations with a typical period of about 40 nm. Our results have direct relevance for modelling this promising class of molecular devices.

The principle of our scanning-gate potential-imaging (SGPI) technique is as follows. An individual semiconducting single-wall carbon nanotube is connected to two metal electrodes, and this transistor is switched to a conducting state by a negative gate voltage, V_g (Fig. 1a). A current flows when a bias voltage, V_b, is applied. At a close distance above the device surface, we scan the tip of an atomic-force microscope (AFM), on which a positive tip voltage, V_t, is applied. The AFM tip acts as a local gate and induces a local potential barrier (Fig. 1b) when it is above the tube. This can reduce the hole current through the nanotube, which is recorded as a function of the tip position (Fig. 1c). The main point of SGPI is that the current reduction depends on the original local potential of the tube. In this way, SGPI maps out the local potential profile of the nanotube.

The top images in Fig. 1d,e show regular AFM images of two different samples with their corresponding SGPI measurements at different bias voltages underneath. The most remarkable feature of these images is that they show a sequence of current dips along the tubes. The dips appear to be confined to the region between the electrodes. Surprisingly, they are rather evenly spaced, with a distance of about 40 nm for the sample in Fig. 1d, and 36 nm for the sample in Fig. 1e. These observations indicate that the edge of the valence band does not vary in a smooth monotonic way. Instead, they point to a potential that is significantly modulated, creating a sequence of barriers for the hole carriers (Fig. 1b). Similar SGPI measurements on metallic tubes did not show any contrast.

The effect of increased bias voltage is illustrated in the lower panels of Fig. 1d,e. The emphasis of the dot pattern appears to shift towards the electrode with the lower potential. Existing dots vanish (particularly clear for very large bias; see Fig. 1e) and new dots appear (bottom right of Fig. 1d; bottom left of Fig. 1e) that were not present for low bias. These trends may be due to the effective gate voltage near the right and left electrodes being different at higher bias voltages. Contrast also diminishes when the tube potential approaches the tip voltage.

The electronic properties of semiconducting nanotubes have been proposed to be sensitive to perturbations by local disorder[2,6–8]. Our results confirm the occurrence of such electronic disorder by direct spatial images. The microscopic origin of this disorder is still unclear, however. The most likely causes are localized charges near the nanotube, or mechanical deformations. Detailed height measurements by AFM did not reveal any correlation between height and electronic features.

Our results shed a new light on other reported transport data. Step features have been found in current–voltage (I–V) curves of TUBEFET devices (ref. 3, and S. J. T. *et al.*, unpublished results). Our findings may explain these observations because an increasing bias voltage can bring down the potential barriers one at a time, leading to step-like features. Reported asymmetries in I–V curves[1,3,4] can now be corroborated by the asymmetries in the potential profile along tubes at low bias. In conduction experiments at low temperatures (ref. 8, and Z. Yao *et al.*, unpublished results), phenomena related to multiple metallic islands have been observed, which can be explained by the barrier sequence seen in our SGPI images. Near the tube on top of the electrodes, no contrast could be found in the SGPI images, even for large tip voltages (up to ±3 V). This indicates that Schottky barriers do not exist at the metal interface, as was suggested earlier[4].

New scanning techniques that give a direct view of the potential landscape, such as the one presented here, provide a promising starting point for a better understanding of the electronic structure of nanotube devices. It should, for example, be feasible to study the effect of deliberate bending of nanotubes, different substrate and electrode materials, and the different geometry of devices such as intramolecular kinked-nanotube diodes[5] and nanotube crossings.

Sander J. Tans*†, Cees Dekker*
**Delft University of Technology, Department of*

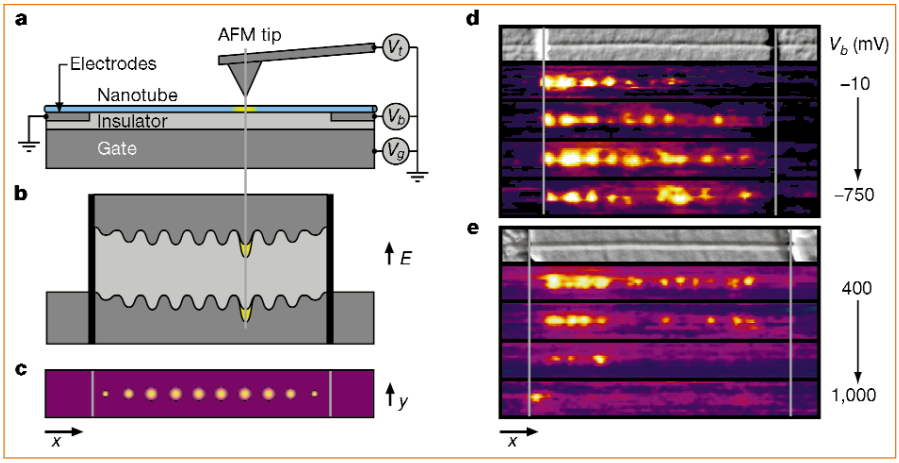

Figure 1 Scanning-gate potential imaging (SGPI) along a semiconducting carbon nanotube. **a,** SGPI measurement set-up. Variable bias voltages, V_b, and a gate voltage, V_g, of −6 V are applied to the TUBEFET device. An atomic-force microscope (AFM) tip at 500 mV is scanned at a constant height of about 10 nm above the surface by retracing each line taken in regular tapping mode AFM while setting a certain height offset and the cantilever amplitude to zero. **b,** Potential landscape of the device. In the conducting state, the valence band edge is horizontal and pinned to the edge of the Fermi level of the electrode[1,9]. The tip voltage creates a potential dip (yellow) which provides a probe for the local potential. SGPI measurements (**d,e**) show that the band edge of the nanotube is not smooth but strongly modulated. **c,** Corresponding SGPI measurement. The device current (colour) is displayed as a function of tip position. Current is reduced when the AFM-tip-induced barrier aligns with minima in the original potential profile. The spatial resolution of the SGPI measurements, which we estimate to be of the order of 10 nm, is determined by the tip–sample distance and the tip radius. **d,** AFM image of the first sample and the corresponding SGPI images for V_b values of −10, −100, −500 and −750 mV (top to bottom). The sample consists of an individual single-wall carbon nanotube (horizontal line) on top of two 25-nm-high platinum electrodes (on the left and right) that are spaced by 650 nm. **e,** AFM image of a second sample and the corresponding SGPI images for V_b values of 400, 500, 700 and 1,000 mV (top to bottom). The sample consists of an individual single-wall carbon nanotube on top of two 750-nm-spaced gold electrodes. The electrodes of this sample are embedded in the SiO_2 substrate to create a flat surface[5] (see **a**).